Molecular BioSystems

Accepted Manuscript

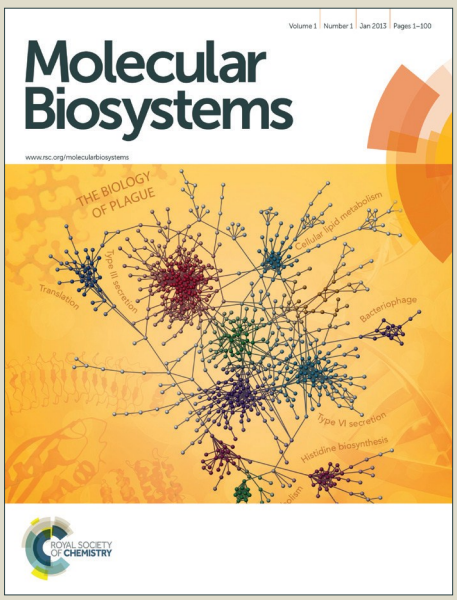

ROYAL SOCIETY OF CHEMISTRY

www.rsc.org/molecularbiosystems

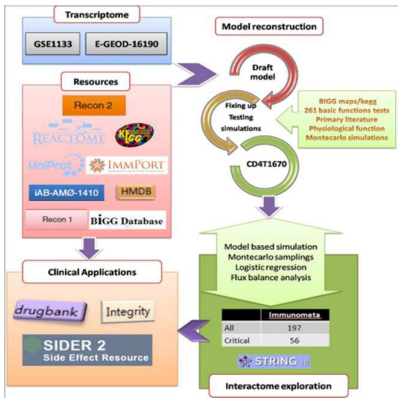

Model-based investigation of metabolism, immunometabolism of CD4+ T cell (CD4T1670) and the application of CD4T1670 in drug development.

Journal Name

ARTICLE

Genome-wide metabolic model shed light on understanding CD4$^+$ T cell metabolically, immunometabolically and in drug design

Received 00th January 20xx,
Accepted 00th January 20xx

DOI: 10.1039/x0xx00000x

www.rsc.org/

Feifei Han[ab], Gonghua Li[a], Shaoxing Dai[a], Jingfei Huang[†acd]

CD4$^+$ T cells play a critical role in adaptive immunity and have been well studied in past decade years. However, the systematic metabolism features are less clear. Here, we reconstructed the genome-wide metabolic network of naïve CD4$^+$ T cells, CD4T1670, by integrating transcriptome and metabolism data. We performed simulations for three critical metabolic subsystems (carbohydrate metabolism, fatty acid metabolism and glutaminolysis). The results were consistent with most experimental observations. Furthermore, we found that depletion of either glucose or glutamine did not significantly affect ATP production and biomass, but dramatically unbalanced the metabolic network and increased the release of some inflammation or anti-inflammation related factors, such as lysophosphatidylcholine, leukotriene and hyaluronan. Genome-wide single gene knockout analysis showed that acetyl-Coa carboxylase 1 (ACC1) was essential for T cell activation. We further investigated the role of immunometabolic genes in metabolic network stability, and found that above 25% of them were essential. And results showed that although PTEN was a well-studied proliferation inhibitor, it was essential for maintaining the stability of CD4 metabolic network. Finally, we applied CD41670 to evaluate side-effects of certain drugs in preclinical experiments. These results suggested that CD4T1670 would be useful in understanding CD4$^+$ T cell and drug design systematically.

Introduction

The CD4$^+$ T cell is one of the major lymphocyte subsets in the adaptive immunity system[1] to respond to various pathogens and co-stimulation. Naïve T cells will activate, proliferate and differentiate into different subtypes to fight pathogens[2, 3]. Among these subtypes, Th1, Th2 and Th17 are effector T cells that mediate immune responses toward the invasion. Treg cells are mainly used to keep all immune process of effector cells under control[4]. Since almost all physiological functions rely on the metabolism, more and more researchers have focused on studies of the metabolic aspects of CD4$^+$ T cells and proposed many strategies of therapy for certain disease[5, 6].

It has been revealed that in naïve T cells, TCA (citric acid cycle) cycle and fatty acids oxidation were mainly used for energy production and other metabolic processes to keep immune surveillance[7, 8]. Upon activation, the metabolic machinery was changed to coordinate this phase transition[9]. Firstly, Warburg effect occurred, also termed aerobic glycolysis, converting pyruvate to lactate even when oxygen was available[10-12]. Secondly, glutaminolysis[8] increased, leading to an increased α-ketoglutarate usage. Thirdly, fatty acid oxidation was down-regulated and lipogenesis increased. Lastly, amino acids and nucleotide metabolism were also increased to meet metabolic needs of the following cell growth and proliferation procedure. Therefore, efficient and rapid biosynthesis and energy supply should be satisfied upon activation.

After differentiation, effector T cells sustain high glycolytic activity and glutaminolytic activity while the Treg use fatty acid oxidation for energy production. When pathogens were cleared, most cells turn to apoptosis, and the rest became memory T cells for responding to future pathogen exposure, whose metabolism was similar to that of the Treg[6]. Therefore, metabolic dysfunction could result in anergy in CD4$^+$ T cells[13].

Although many efforts have been put on metabolism in CD4$^+$ T cells, more detailed mechanisms are still unknown. This is partly due to the limitations of experimental techniques. Thus the trials to reach clinical purposes by interfering metabolism are very limited. In silico modeling and simulations could rightly make up for this vacancy and help to guide experimental design. To this end, we firstly reconstructed the metabolic network of naïve CD4$^+$ T cells, CD4T1670. Secondly, we explored in detail the three mostly fundamental pathways: basic carbohydrate metabolism, fatty acid metabolism and glutaminolysis by in silico simulations. We found that depletion

[a] State Key Laboratory of Genetic Resources and Evolution, Kunming Institute of Zoology, Chinese Academy of Sciences, 32 Eastern Jiaochang Road, Kunming, Yunnan 650223, China
[b] Kunming College of Life Science, University of Chinese Academy of Sciences, Beijing 100049, P.R. China
[c] KIZ-SU Joint Laboratory of Animal Models and Drug Development, College of Pharmaceutical Sciences, Soochow University, Suzhou 215123, P.R. China
[d] Collaborative Innovation Center for Natural Products and Biological Drugs of Yunnan, Kunming 650223, P.R. China
†.Corresponding author: Jingfei Huang
State Key Laboratory of Genetic Resources and Evolution, Kunming Institute of Zoology, Chinese Academy of Sciences, Kunming 650223, P.R. China
Fax: +86-0871-65199200; Tel: +86-0871-65199200; E-mail: huangjf@mail.kiz.ac.cn
Electronic Supplementary Information (ESI) available. See DOI: 10.1039/x0xx00000x

of either glucose or glutamine did not significantly affect ATP production and biomass, but dramatically unbalanced the metabolic network and increased the release of some inflammation or anti-inflammation related factors, such as lysophosphatidylcholine, leukotriene and hyaluronan. Genome-wide single gene knockout analysis showed that acetyl-Coa carboxylase 1 (ACC1) was essential for T cell activation. Reaction markers were identified for each condition under inspection. Thirdly, related metabolic genes were screened out for glucose, glutamine depletion and lipogenesis inhibition. And HIV-1 infection was taken as an example to prove that the prediction power of the model-based simulation was acceptable. Fourthly, we further investigated the role of immunometabolic genes in metabolic network stability, and found that about 28% (56 out of 197) of them were essential. And PTEN were presented in details. Finally, we presented an application of CD4T1670 in drug design and side-effects evaluation.

Materials and methods

Data sources and preliminary processes

1, Transcriptome data for $CD4^+$ T cell

Cell-specific gene expression data using the next generation sequencing technique were downloaded for $CD4^+$ T cell(E-GEOD-16190)[14] from EBI ArrayExpress Archive. Only data of $CD4^+$ T cells from a healthy donor were used.

Data were processed as described in previous studies[15,16]. We obtained the FPKM(Fragments Per Kilobases of exon per Million fragments mapped) value for each transcript for determining present/absent calls in the following reconstruction process.

2, Enzymic drug target and corresponding drugs were obtained from Drugbank database[17]. Then we extracted corresponding entries that expressed in $CD4^+$ T cells. Then we downloaded side effect data of drugs from SIDER 2, the side effect resource (http://sideeffects.embl.de/)[18], which records information on marketed medicines and their adverse effects.

3, The human global metabolic network reconstructions, recon1 and recon2 were obtained from their original published papers[19, 20]. Compartmentalized metabolic maps were downloaded from the BIGG database[21]. Reference metabolic pathways were retrieved from KEGG (kyoto encyclopedia of genes and genomes) database (www.kegg.jp/). Proteome data on lymph node and spleen in HPA (www.proteinatlas.org) [22, 23] and GSE1133 published gene expression data in blood $CD4^+$ T cells[24] were referred to determine the expression status for some dubious metabolic genes. In other words, for metabolic genes with low expression in E-GEOD-16190 were checked with their expression status in GSE1133 and HPA.

4, Databases on metabolism, such as HMA (www.metabolicatlas.com), HMDB (www.hmdb.ca/) and TransportDB (www.membranetransport.org) were used for correcting the formula or other related information for some incorrect reactions.

Metabolic network reconstruction and validation

The reconstruction was derived from Recon2, a global human metabolic network[19] using GIMME algorithm[25]. Recon2 consists of 2194 ORFs, 7440 reactions and 5063 metabolites in total. GIMME, Gene Inactivity Moderated by Metabolism and Expression, is one of the most popular algorithms for pruning the global metabolic network by integrating cell-specific gene expression data. As inputs, GIMME requires: 1) the genome-scale reconstruction, recon2; 2) a set of two-value gene expression data, in which 0 represents absent calls and 1 represents present calls; and 3) one or more required metabolic functionalities (RMF) that the cell is assumed to achieve, and which also can be set to all reactions. GIMME is available in a matlab package, the COBRA Toolbox v2.0[26]. Here the $CD4^+$ T cell expression data was mapped to the Recon2 reactions and it resulted in a draft model. This model was then reconciled with the maps in BIGG database, KEGG database, HPA data, GSE1133 data[24], uniprot, and others.

As shown in Figure 1, we firstly removed dead-end reactions and metabolites. Necessary transport and exchange reactions were then added for maintaining connectivity of this network. Secondly, we set exchange constraints for 71 reactions (supplementary Table 1) based on the published functional macrophage model, iAB-AM@-1410[27] due to the sparse of corresponding data directly on the $CD4^+$ T cells. Thirdly, network connectivity was tested and 261 out of 288 basic metabolic functions of a cell, published with the recon1 model[20]. The reconciling process was iterated, for every change we do to the network, network connectivity and basic functions had to be checked. Biomass function, ATP synthesis function were treated as target function during the testing iteration. Finally, we got our curated model and used it for following simulation and analysis processes.

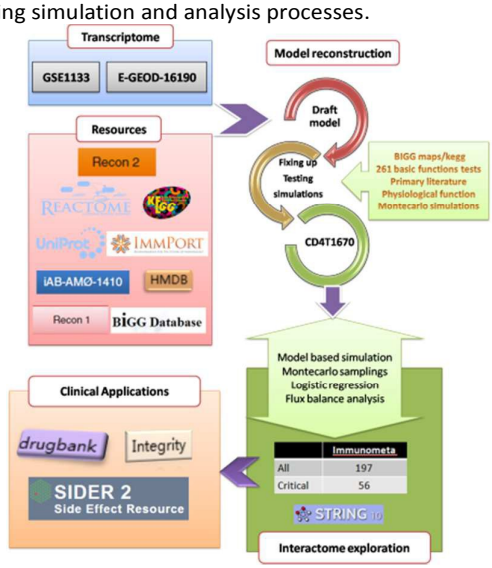

Figure 1 Flowchart of this work. Firstly, transcriptome data were processed to get absent/present calls of metabolic genes. Recon2 was tailored to naïve $CD4^+$ T cell specific model and this model was modified and validated with multiple sources of data. Secondly, the final naïve model was characterized with its metabolic features by flux balance analysis and monte-carlo sampling methods. Thirdly, immunometabolic genes and their

metabolic functions were investigated in silico and PTEN was presented in details both metabolically and immunologically. Finally, $CD4^+$ T cell expressed enzymatic drug targets and corresponding drugs were extracted from DrugBank and drug side effects information was obtained from SIDER2 database. And we investigated the effects of these drug targets on the metabolic model and correlated their actions with side effects of their drugs and proposed the application of the metabolic network in drug design and side effects evaluation.

Immunological analysis of $CD4^+$ T cells and identification of immunometabolic genes

Immunological genes and proteins were downloaded mainly from two databases: InnateDB[28] and Immprot[29]. A total of 6363 genes were retrieved and only the genes expressed in the $CD4^+$ T cell were remained. The remained immunological genes were then used to find overlaps with $CD4^+$ T cell metabolic network, noted as immunometabolic genes. Single gene deletion was performed for each immunometabolic genes as well as pure metabolic genes using COBRA toolbox in matlab. Affected reactions and their metabolic functions were identified for further comparative analysis. An immunological network for $CD4^+$ T cell was built using all expressed immunological genes using cytoscape3.2.1 and one of its plugins, GeneMania. Genetic interactions, physical interactions, transcriptional factor targets, consolidated pathways, miRNA target predictions and InterPro were used in the construction. And we didn't incorporate information from predictions. This network, together with the reconstructed CD4T1670, was used to analyze the properties of $CD4^+$T cell expressed immunometabolic genes.

Monte-Carlo sampling and logistic regression

To get the feasible flux distributions for all reactions in the $CD4^+$ T cell model, Monte Carlo sampling was conducted. Considering the network size, unbiased sampling can be very much time-consuming, so a modified version, ACHR (artificially centered hit and run) algorithm was used instead[30]. Here in our case, we calculated 10000 warmup points and 10000 sampling points for each condition. Sampling errors were calculated and points with error greater than 1e-8 were removed for a balanced control of all the sampling results. Before comparison between sampling results of different models, we normalized all sampling data points, and then a paired T-test assuming that data from different conditions have unknown and unequal variances was performed. False discovery rates were then calculated by the method introduced by Benjamini and Hochberg to control the use of the linear step-up (LSU) procedure. Significance level was set as 0.05. And considering the sensitivity of metabolic reactions, those with flux fold changes (log2 transformed) over 1 were considered as differentially expressed. Moreover, reactions with fluxes of changed direction were also kept. And only reactions with flux value over 1e-6 were identified as functional.

Logistic regression was conducted to determine the weight of each reaction to feature the transformation of cells' functional states. Top 10th percentile items were used as reaction markers under certain perturbation.

Results and discussion

Gene expression profile analysis

Before reconstruction, cell-specific gene expression data using the next generation sequencing technique were obtained for $CD4^+$ T cell from NCBI Gene Expression Omnibus and EBI ArrayExpress Archive. We processed raw data, extracted FPKM value for each transcripts and used them in the following reconstruction process.

Since the reconstruction procedure required presence and absence calls for each gene/transcript based on the expression data, we firstly calculated the FPKM distribution of all data obtained above. Result showed that the distribution of gene expression values is extremely skewed right (the median and mean FPKM values are 0.0815 and 17.6949; the bottom 25th percentile of FPKM values is 0, and the top 25th percentile of FPKM values is 2.6517; the minimum FPKM value is 0 and the maximum FPKM is 3.4130e+004). Here we used a similar logic as described in Toung's work[31] and take genes whose FPKM values were less than 0.0815 as low expression genes and those with FPKM values above 17.694 as highly expressed genes. The expression statuses of low and medium expressed genes were validated with HPA data, GSE1133 and others. Present/absent calls for metabolic genes were used in the following reconstruction process.

Reconstructed naïve $CD4^+$ T cell model: CD4T1670

The reconstruction is derived from the recently published global human metabolic network, Recon2[19]. We firstly tailored the global network to the draft CD4 model with the GIMME algorithm[25].

Table1 Overview of basic features of CD4T1670, recon2 and iAB-AM@-1410.

	iAB-AM@-1410	Recon2	CD4T1670
Transcripts	1410	1789	1670
Reactions	3394	7440	4229
Metabolites	2583	5063	3310(1843)
GARs*	67.8%	59.9%	78.3%

* GARs, gene associated reactions

Table2 Subcellular statistics of CD4T1670

Subcellular location	Reaction count	Metabolite count
Cytosol	999	991
Mitochondria	457	518
Lysosome	187	225
Golgi apparatus	181	231
Nucleus	112	145
Reticulum	253	334
Peroxisome	286	357
Extracellular	303	301

Massive curation works were done by integrating data from multi-sources of data as described in material and methods. 1, The obtained network was with many reaction gaps and errors about reaction directions and the lower and upper bounds. We detected reaction gaps and performed gap-filling by integrating KEGG pathways, BIGG maps, existing macrophage model[32] and adipocyte model[33]. And then we modified incorrect reaction directions (and reversibility) and reaction bounds accordingly. To test the metabolic functionality of the draft network, we assessed the ability of the networks to complete metabolic functions in Recon1[20], which was one of the main steps in the network gap filling and validation procedure used in other reconstruction studies[32, 33]. Here we performed 261 tests and 115 were passed (supplementary Table 1), indicating that the model we've constructed doesn't possess all features of a global network and thus was tissue specific. 2, Energy generation, fatty acid metabolism, glutaminolysis and other tests also performed and validated with existing experiments data for model curation. 3, Finally, we adjusted the maximum flux of biomass generation to be 0.032 mmol gDW^{-1} hr^{-1}. And it indicated a constraint of the whole network was functional. Till now, a functional and constrained model was ready for further analyses (CD4T1670 was available in supplementary as CD4T1670.xml and CD4T1670.xls).

The contents of the final CD4T1670 network compared with Recon2 as well as iAB-AM@-1410 are shown in table1. And information on subcellular models is shown in Table2.

Metabolic features of naïve $CD4^+$ T cell

Carbohydrate metabolism

In normal condition, aerobic respiration is mainly used for energy production. This involved two key metabolic pathways: glycolysis and TCA cycle. This is the same for naïve $CD4^+$ T cells, although both pathways occurred on a relatively low level. Previous studies have found that upon T cell activation, a metabolic transition to aerobic glycolysis (lactate is produced from glycolytic pyruvate, even when oxygen is sufficient) occurred[34], similar to the Warburg effect observed in cancer cells[35]. To activate the T cells, expression of glucose transporter glut1 and its translocation to the cell surface increased and lead to increased glucose uptake[36].

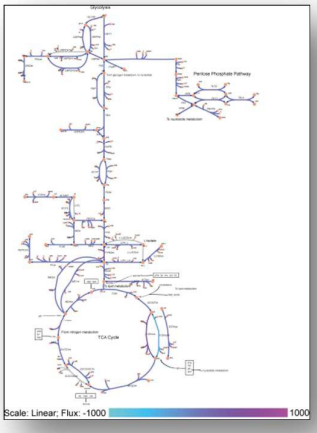

Figure 2 Fluxes of reactions in the key carbohydrate metabolism of naïve CD4T1670. Flux values were from monte-carlo samplings. Mean flux of each reaction was casted at the BIGG map. Flux range is -1000 to 1000 and is indicated by color scope from cyan to purple. Metabolites that linked with boxes were nodes in the pathway that connected with other metabolic pathways (metabolites in boxes were nodes from these pathways).

To see how the reconstructed metabolic model responded to glucose metabolism, we closed all glucose transport reactions to simulate the glucose depletion condition and then performed monte-carlo sampling. Result showed that fluxes of most reactions in glycolysis and TCA cycle were kept at a low level in normal naïve CD4T1670 (Figure 2). ATP generation through oxidative phosphorylation was with an average flux value of about 0.5219 mmol gDW^{-1} hr^{-1}, and biomass production was 0.0014 mmol gDW^{-1} hr^{-1}. This indicated the relatively low energy and metabolic state of this cell as mentioned above.

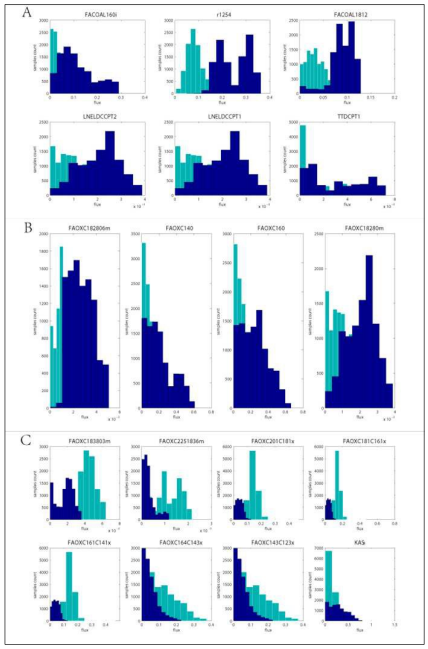

Figure 3 Flux changes of reactions on fatty acid metabolism when glucose was depleted. A presented some decreased reactions on fatty acid oxidation or transport; B presented some of those decreased fatty acid oxidation reactions in mitochondria; C showed increased fatty acid oxidation reactions in peroxisome and the decreased reaction, KAS8, for de novo fatty acid synthesis. The flux distributions in normal condition and glucose blocked condition were shown with blue box and cyan box, respectively.

After glucose depletion, 597 reactions were significantly differentially expressed (flux>1e-6 mmol gDW^{-1} hr^{-1}; pvalue<0.05; absolute fold change>=1, log2 transformed). Among these, 265 reactions were downregulated, 243 were upregulated and 89 were with reversed flux. Interestingly, we observed that glycolysis and TCA cycle were not dramatically affected. This proved the result of Macintyre's study that

GLUT1, the key transporter of glucose in vivo, was not required for naïve T cells' survival[37]. In support of this, flux through biomass reaction was not changed and ATP generation through oxidative phosphorylation was with an average flux value about 0.411 mmol gDW^{-1} hr^{-1} (a slight decrease). Many reactions on glycan degradation were upregulated, although they still ran on a low level. For example, reactions in keratan sulfate degradation and chondroitin sulfate degradation in lysosome were upregulated. Besides, in normal condition, glucose could transport from cytosol to endoplasmic reticulum. But when glucose was removed from the extracellular environment, the transport reaction reversed. Thus, we supposed that the barely affected glycolysis might temporally attribute to the filling from other carbohydrate pools. Even under those changes, glycan metabolism was still disturbed since increased degradation would affect many functions which were important for the cell, such as the cytoskeleton or glycosylation of proteins.

Moreover, fatty acid metabolism was greatly affected both in mitochondria and peroxisome. Firstly, fatty acid activation in cytosol was significantly decreased (Figure 3A) and so was the transport of activated fatty acid into mitochondria. Secondly, beta oxidation of long chain fatty acids such as tetradecanoate (n-C14:0), palmitate (n-C16:0), linolenic acid (n-C20:6), linoelaidic acid (n-C18:2) and docosa-pentaenoic acid (n-C22:0) (Figure 3B) was decreased in mitochondria. Thirdly, although beta oxidation of certain fatty acids in mitochondria was also increased, the upregulation was more remarkable in peroxisome (Figure 3C). And because many of them were O2 involved and h2o2 generation would increase. Fourthly, de novo lipogenesis was inhibited (KAS8, Figure 3C) while uptake of some fatty acids increased, such as linolenic acid and hexadecanoate. These metabolic changes on fatty acid metabolism were very much similar to that of the differentiation to Treg cells from activated $CD4^+$ T cell. It is mainly because differentiation of Treg cell doesn't rely on the glycolytic-lipogenic pathway[38]. On the contrary, effector T cells generation requires high glycolytic and lipogenic activities and extracellular supply of extra fatty acid could not reverse the effects of inhibition to these two pathways[39]. The results indicated that glucose depletion would impair the normal immunological function of $CD4^+$ T cell by inhibiting the differentiation of effector T cells metabolically.

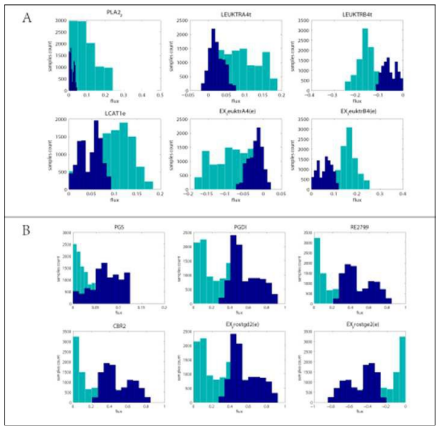

Figure 4 Flux changes of reactions about some inflammatory metabolites when glucose was depleted. In A, PLA2_2 is the reaction for lysophosphatidylcholine generation and the rest reactions were for leukotriene uptake or transport; B showed downregulated reactions for prostaglandin metabolism. The flux distributions in normal condition and glucose blocked condition were shown with blue and cyan histograms, respectively.

Furthermore, we detected changes of certain inflammatory factors (Figure 4). And we found that releases of leukotriene and lysophosphatidylcholine were increased and leukotriene was also turned from being taken up to being released. But prostaglandin synthesis was decreased. So metabolic disorder resulting from glucose removal could cause inflammatory outcomes. But the mechanism of the different actions of those inflammatory molecules observed here were not clear.

We performed logistic regression to identify all glucose-associated factors. Top 10 percentile of reactions markers were selected out. Results showed that about 30 different metabolic functions were relevant (supplementary Table 2). These functions covered amino acid metabolism, fatty acid metabolism, nucleotide metabolism, carbohydrate metabolism, folate metabolism and exchange or transport reactions. This indicated a significant reorganization of the normal metabolic system and thus the abnormality of the $CD4^+$ T cell.

To sum up, altered pathways such as fatty acid oxidation and glycan metabolism could prevent T cell from dying when glucose was totally depleted. So glucose is not indispensible for survival of $CD4^+$ T cells. However, significant metabolic disturbance occurred, inflammatory factors were released and these might finally result in malfunctions of $CD4^+$ T cell and other tissues.

Glutamine metabolism

Glutamine is abundant in serum, and there were studies showing that lymphocytes consume glutamine at a comparable rate to glucose[40]. T cells are highly sensitive to glutamine metabolism, which is required for T cell activation and effector T cell development[41]. And T cell proliferation could be impaired by glutamine deletion[42]. Since cell size and protein synthesis rates of T cells were all increased upon activation[35], T cell activation required oxidative phosphorylation for energy production. However, rapid induction of aerobic glycolysis was also needed not only for fast ATP generation, but also supplying metabolic intermediates for the syntheses of other biomolecules such as lipids, carbohydrates, proteins, and nucleic acids[11]. We already know that a key component of TCA cycle, a-ketoglutarate, is the metabolite for glutamine through glutamate to enter the energy production pathway. Glutamine can also serve as an amine group donor for nucleotide synthesis. Thus, glutamine metabolism is indispensible for $CD4^+$ T cell.

To see how glutamine functions in T cell and if the termination of extra glutamine supplying will generate features preventing $CD4^+$ T cells from activation, we closed glutamine related transport/exchange reactions in CD4T1670. And results

showed that top 5 percentile (210 reactions) of highest weights were mostly corresponding to amino acid transport or exchange reactions (159 reactions), indicating a dramatic disturbance to the amino acids balance. This was consistent with results from Erkka's study[41] in which strongest inhibitions of all other amino acids were observed upon glutamine depletion. Other 52 affected functions were showed in supplementary Table 3, within which we could found more closely related factors that were important for or related with glutamine metabolism.

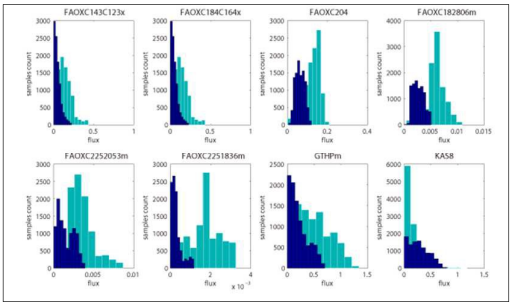

Figure 5 Flux changes of some reactions in fatty acid metabolism system upon glutamine depletion. FAOXC143C123x, FAOXC184C164x, FAOXC204, FAOXC182806m, FAOXC2252053m, FAOXC2252053m and FAOXC2251836m were some reactions on fatty acid oxidation in either mitochondria or peroxisome. KAS8, is one of the most critical reactions for de novo fatty acid synthesis. And GTHPm is the reaction occurring in mitochondria for eradicating H2O2. The flux distributions in normal condition and glucose blocked condition were shown with blue and cyan histograms, respectively.

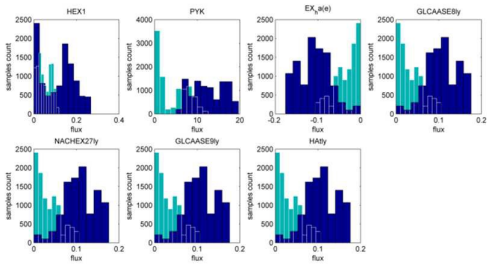

Figure 6 Flux changes of some reactions in glycolysis and hyaluronan metabolism upon glutamine depletion. HEX1 and PYK were two critical reactions in glycolysis while the rest were reactions in hyaluronan metabolism. The flux distributions in normal condition and glucose blocked condition were shown with blue box and cyan box, respectively. The flux distributions in normal condition and glutamine blocked condition were shown with blue and cyan histograms, respectively.

From supplementary Table 3, we observed that fatty acid metabolism was also a key factor related to glutamine metabolism. After further investigation, we found that most fatty acid oxidation reactions both in mitochondria and peroxisome were dramatically upregulated (some were presented in Figure 5) but de novo lipogenesis were significantly downregulated (Figure 5, KAS8). Similar to that of peroxisome, H2O2 generation in mitochondria was significantly increased. This could be indicated not only from lipolysis reactions, but also the reaction to eradicate H2O2, GTHPm (in Figure 5). Although fatty acid oxidation increased and its final product, acetyl-Coa, could fill the TCA cycle and maintain energy production and anabolism on a certain level, we observed that glycolysis was inhibited. This was due to the significantly downregulated HEX1 and PYK (Figure 6). HEX1 was the initiating reaction of this pathway, and PYK was the second ATP production reaction. Compared with the results of glucose depletion, the inhibited glycolysis upon glutamine starvation further supported the idea that glutamine metabolism played critical roles in $CD4^+$ T cell.

In addition to the results above, we also found that hyaluronan (HA) degradation was greatly decreased (Figure 6). This meant a relatively higher level of high molecular weight HA extracellularly and lower level of low molecular weight HA. Actually, when glucose was depleted, HA degradation was also decreased. There are already studies showing that HA in the matrix environment acts as a link between the innate inflammatory network and the regulation of adaptive immune responses. Intact HA functions to enhance the inflammation-suppressive effects of activated Treg cells while its degraded, low molecular weight forms promote inflammation and angiogenesis when infection and injury occur[43-45]. So, the relatively decreased high molecular weight HA degradation, which in other words, a relatively increase of extracellular HA observed here, might functioned to counter inflammatory effects caused by glutamine or glucose starvation. This might indicate a self-protection strategy of our body in response to nutrition starvation.

As mentioned above, glutamine depletion could result in inflammatory outcome. This was because that releases of lysophosphatidylcholine and leukotrieneA4 were increased and prostaglandin synthesis (Figure 7) was decreased as they showed in glucose depletion.

Moreover, inositol phosphate metabolism was also affected. Since PI3K-Akt-mTOR pathway is critical in regulating the functional states of $CD4^+$ T cell, the changes could affect the signaling transduction. This could render activation failure and impaired immune response. Erikka and coworkers also found that glutamate supply could not reverse the effects of glutamine depletion[41]. And we also increased glutamate uptake otherwise, and results were well agreed with the result of Erikka's result (data not shown).

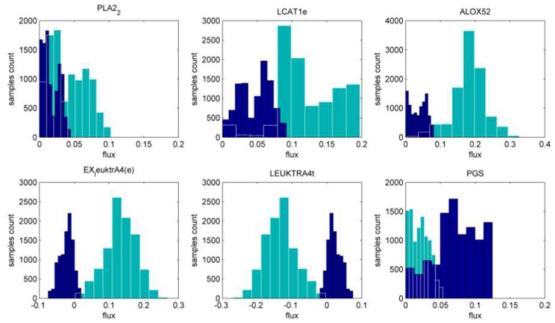

Figure 7 Flux changes of some reactions around some inflammatory molecules upon glutamine depletion. PLA2-2 is the reaction for generating

lysophosphatidylcholine; LCAT1e, ALOX52, EX_leuktrA4, and LEUKTRA4t are reactions responsible for leukotrieneA4 transport or metabolism; and PGS is the reaction for prostaglandin generation. The flux distributions in normal condition and glutamine blocked condition were shown with blue and cyan histograms, respectively.

All results indicated that, similar to glucose metabolism, glutamine metabolism was very important in maintaining normal functions of $CD4^+$ T cells and disruption of it could result in inflammatory[46-52] and more outcomes. Glutamine is not a necessary amino acid for human and can be synthesized intracellularly. However, the roles it plays in amino acid metabolism, nucleotide metabolism, energy metabolism, inflammation and other subsystems in $CD4^+$ T cells suggest that keeping serum glutamine on a stable concentration is important to maintain health.

Fatty acid metabolism

It has been proved that naïve T cells use not only glycolysis and TCA cycle, but also fatty acid oxidation to fuel oxidative phosphorylation[7]. And fatty acid metabolism plays a critical role in determining the fate of T cell subsets[39]. ACC1, the key enzyme of fatty acid synthesis in cytosol has been proved to be important for T cell immunity[53, 54]. Its inhibition could not only directly block de novo fatty acid synthesis, but also result in the reorganization of cellular metabolic network[39]. And these metabolic changes could finally affect the transformation behavior of activated $CD4^+$ T cells to their subsets.

Here we inhibited ACC1 by setting the flux of its catalyzed reaction, ACCOAC, to zero in CD4T1670 and analyzed the effects of this perturbation on the whole metabolic system. We extracted the top 10 percentile of reaction factors (423 reactions) and functional classification showed that except for exchange and transport reactions, 29 kinds of metabolic functions corresponding to 152 reactions were selected out (Supplementary Table 4).

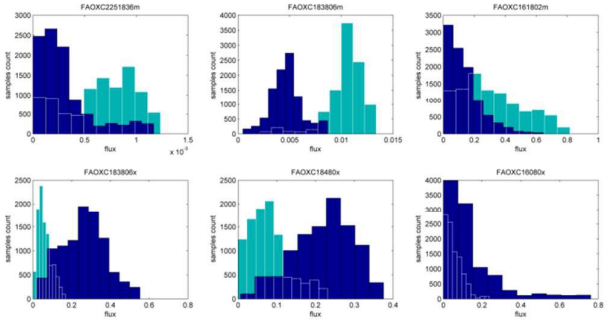

Figure 8 Flux changes of some reactions in fatty acid metabolism system upon acc1 inhibition. FAOXC2251836m, FAOXC183806m and FAOXC161802m were three of upregulated fatty acid oxidation reactions in mitochondria. FAOXC183806x, FAOXC18480x and FAOXC16080x were three of downregulated fatty acid oxidation reactions in peroxisome. The flux distributions in normal condition and acc1-inhibited condition were shown with blue and cyan histograms, respectively.

We firstly inspected the changes in fatty acid metabolism. Results showed that lipogenesis was dramatically inhibited and fatty acid oxidation in mitochondria was mostly upregulated while that in peroxisome was mostly downregulated (Supplementary Table 4, Figure 8). Most h2o2 generation reactions in peroxisome were downregulated, implying a decreased h2o2 production. Interestingly, we found that the reaction for removing h2o2 in mitochondria, GPTHm, was significantly downregulated (foldchange=-1.13). This reaction takes h2o2 and reduced glutathione as inputs. Since the reaction for generating reduced glutathione or other reactions consuming glutathione were not dramatically affected, we deduced that mitochondria production of h2o2 decreased. And this implied a release of oxidative stress in the cell. There were already studies showing that increased fatty acid oxidation could protect microphage from ROS damage[55], and here we found that the increase of fatty acid oxidation after lipogenesis inhibition could also reduce ROS damage to $CD4^+$ T cells. Even through, $CD4^+$ T cell would unable to be fully activated, since fatty acid synthesis was required for this process[7, 8, 39]. Besides, fatty acid uptakes were mostly downregulated as shown in Figure 9. And we also observed increases in glutamine and glucose uptake. As showed in Figure 2, citrate was the node that linked lipid metabolism and TCA cycle. Intracellular starvation of lipid might push the flux to this direction and disturbance of amino acids and nucleotides metabolism (supplementary Table 3) also exerted pressures on the TCA cycle. So increased uptake reactions of glutamine and glucose might be compensations for this intracellular imbalance caused by lipid starvation.

Furthermore, inflammation related reactions were also inspected and just like those in glucose and glutamine depletion, lysophosphatidylcholine and leukotriene releases were also increased. And this might indicate an inflammation outcome resulted from fatty acid metabolism disorder in $CD4^+$ T cells.

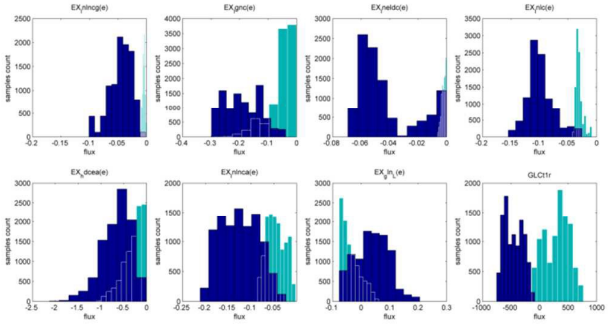

Figure 9 Flux changes of some uptake reactions for fatty acids and others upon acc1 inhibition. The first 6 reactions were uptake reactions for different fatty acids which all showed decreased uptake rates. The last two reactions were uptake reactions for glutamine and glucose respectively and both of them was with increased uptake rates. The flux distributions in normal condition and acc1-inhibited condition were shown with blue and cyan histograms, respectively.

To sum up, we had deeply investigated three critical metabolic subsystems in $CD4^+$ T cell, carbohydrate metabolism, glutamine metabolism and fatty acid metabolism. We found that these three functions were closely associated. And

disruption of any one of them could affect others and functions beyond. Interestingly, we found that peroxisomal fatty acid oxidation in $CD4^+$ T cell was very sensitive to perturbations from either intracellular or extracellular metabolic changes. We know that peroxisomal lipid substrates do not contribute much to energy production[56]. So we deduced that the sensitivity of peroxisomal fatty acid metabolism and h2o2 production might be important to buffer metabolic stress of $CD4^+$ T cell and protect mitochondria from instant ROS stress in some extent. This might then protect our body from inflammation or loss of $CD4^+$ T cells when malnutrition occurs for a short time and maintain flexibility of our immune system. This also implied to us that modulation of peroxisomal functions might reach clinical targets in the future. Besides, we found that any perturbation to the metabolic network could result in inflammatory outcomes. And we found that any disruption resulted reorganization of the $CD4^+$ T cell metabolism might have the risk of activation failure and affect the adaptive immunity function. So, the model we built could be used to simulate conditions of malnutrition and predict corresponding effects. This can be used to guide healthy dietary decisions.

Gene markers identification and applications

In addition to identifying reaction markers related with glucose depletion, glutamine depletion and acc1 inhibition, we further identified associated gene markers (supplementary Table 2-4). For the top 10 percentile of reactions, 145, 123 and 163 genes expressed in $CD4^+$ T cell were obtained respectively and Figure 10 was an overview of the overlap of these 3 groups. After annotation using DAVID, diseases associated with the functional abnormalities of those genes were identified. For glucose depletion, about 74 affected genes were found to be related with at least one type of disease or abnormality (supplementary Table 2). And among these, 11 genes could interact with HIV-1, the human immunodeficiency virus 1. In the case of glutamine depletion, 57 genes were identified to be disease-related (supplementary Table 3). And 7 genes could interact with components of HIV-1. And after acc1 inhibition, 79 possibly affected genes were associated with different kinds of diseases (supplementary Table 4). Twelve of them could interact with components of HIV-1.

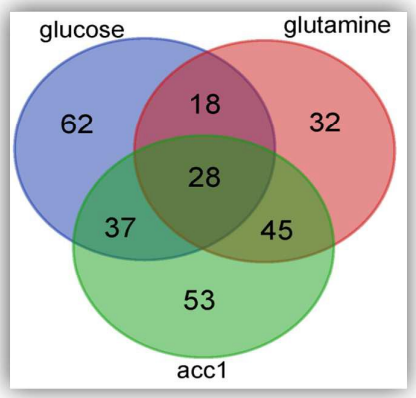

Figure 10 Venn diagram displaying related genes for marker reactions of glucose, glutamine and acc1 depletion respectively, and their overlaps. Top 10 percentile of reaction markers associated genes for each case were included in the analysis.

Other than other type of diseases, the main host of HIV-1 is $CD4^+$ T cell. So we examined our predicted results with transcription and existing data on metabolic changes upon HIV-1 infection. From perturbation tests of above, we identified 17 genes that were both relevant with one or more kinds of basic metabolic functions of $CD4^+$ T cell and could interact with HIV-1. Of the 17 genes, 15 (88%) were found to be significantly up- or down- regulated in other dataset due to HIV-1 infection(Table 3). We already know that glycolysis was increased and required by HIV-1 infection[57, 58], beta oxidation of fatty acid in mitochondria could barely happen[58], and amino acid and nucleotide were both reorganized to satisfy the demands of HIV replication[58, 59]. Those genes we found here and their corresponding reactions could be important in explaining the mechanism of metabolic transformation caused by HIV-1 infection. Besides, genes that didn't interact with HIV-1 but responded to the infection were also considered to be important. For the three cases, 67 (38.6%), 52 (42.3%) and 70 (43%) genes were found to be differentially expressed upon HIV-1 infection, respectively. Since the simulation here was based on single factor perturbation, and infection was a more complicated process that involved many factors, results we got here were considered acceptable. And multiple variables based investigation on HIV-1 infection and how those factors acted in the infection would be presented otherwise and not the topic of this work. So, we proposed that in silico simulation using CD4T1670 should be very useful in studying the mechanism of certain disease metabolically through in silico perturbations.

Table 3 17 genes identified from in silico perturbation which could interact with HIV-1

ID[a]	GENE	HIV_INTERACTION	glc	gln	acc 1	hiv infection[d]
2821	GPI	env: gp120,	1[b]	0[c]	1	down
1374	Cpt1a	env: gp160,	1	1	1	down
1375	CHKB	env: gp160,	1	1	1	down
6520	SLC3A2	env: gp160,	1	1	1	down
8140	SLC7A5	env: gp160,	1	1	1	down
126129	Cpt1c	env: gp160,	1	1	1	NA[e]
2203	Fbp1	gag:matrix,	1	0	0	up
8789	FBP2	gag:matrix,	1	0	0	up
5105	PCK1	pol:integrase,	1	0	0	up
57379	AICDA	vif:Vif,	1	0	0	up a little
291	SLC25A4	vpr:Vpr,	1	0	1	down a little
2879	GPX4	tat:Tat,	0	1	0	down
1376	cpt2	env: gp160,	0	1	1	down
10632	ABCC1	tat:Tat,	0	0	1	down

4907	Pla2g2a	env: gp120,	0	0	1	NA
522	ada	env: gp120,	0	0	1	down
137872	pla2g6	env: gp120,	0	0	1	up a little

a: the entrez id of a gene; b: 1 means this gene is identified in this perturbation test; c: 0 means this gene was not identified in this perturbation test; d: Information about this aspect was collected from the study of Chang's[60]; e: NA means that this gene was not related HIV-1 infection.

Unlike HIV-1 infection, other diseases' information might derived from data in other tissue/cell type, and not directly related with $CD4^+$ T cell. Till now, many tissue-specific metabolic networks have been published, such as liver[61], adipocyte[33], heart[62], kidney[63], macrophage[32] and so on. Model-based simulations can be used to investigate interactions of multiple tissues or cells. Considering the critical role of $CD4^+$ T cell in immunity and metabolism of our body, we propose that in silico investigations on the interactions among those networks will greatly help with our understanding the ways our body works and how disease progresses. And the CD4T1670 model will help to lay foundations on such studies.

Interface of metabolic functions and immunological functions

$CD4^+$ T cell is one of the most important members of human adaptive immune system. Here we explored the interface of the immunological functions and its metabolic basis based on the CD4T1670. Immunological data was mainly from two databases: InnateDB[28] and Immport[29]. The final count of integrated immunological genes was 6363. We found that about 2201 immunological genes were expressed in $CD4^+$ T cells and 197 genes were overlapped with genes of our metabolic network. Function enrichment of immunometabolic genes in $CD4^+$ T cells was conducted and terms with corrected p value less than 0.05 were displayed in Figure 11. We can see that these immunometabolic genes participated in many important pathways for cell activation, proliferation, immunological functions and so on. And they are mainly involved in carbohydrate, lipid and nucleotide metabolism.

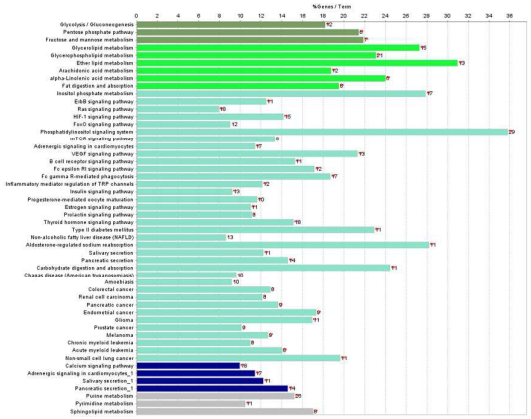

Figure 11 Function enrichment results of immunometabolic genes in $CD4^+$ T cells. Terms in the same color belong to a same function group. The number on each bar stands for how many immunometabolic genes in $CD4^+$ T cell enriched in this term. And x axis shows the ratio of immunometabolic genes in $CD4^+$ T cell to all genes in this term.

To see how these immunometabolic genes function in the metabolic network and to reveal the metabolic basis of their immunological functions, we performed single gene deletion for each immunometabolic gene in CD4T1670. We found that 56 (about 28%) genes' deletions could disrupt the steady state of the network (Figure 12, supplementary Table 5). For each deleted gene, we analyzed the properties of its affected reactions and extracted the metabolic subsystems they belonged. Besides, we constructed the immunological interaction network for $CD4^+$ T cell using the 2141 immunological genes. Immunometabolic genes were located and the number of interactions for each of the 56 selected genes and the rest 141 genes were compared. Besides, we randomly selected 100 immunological genes in the immunological interaction network and 200 metabolic genes within which 39 deletions could disrupt the balance of the network for comparison.

Firstly, we compared the immunometabolic genes and randomly selected simple metabolic genes, all of which could affect the balance of the metabolic network upon deletion. Means and standard errors of up-regulated, down-regulated and direction reversed reactions were calculated for both cases. Affected metabolic functions were also extracted for comparison (data not shown). And we found that deletions of two groups of genes didn't show big differences in the number of metabolic subsystems. Then we compared immunometabolic genes and randomly selected pure immunological genes in the constructed immunological network. Direct linked nodes and related interactions around the target gene were extracted. Similarly, no significant changes were detected between two groups (data not shown). Both results suggested that, immunometabolic genes didn't work different topologically with either pure metabolic genes in the metabolic network or pure immune genes in the immunological network.

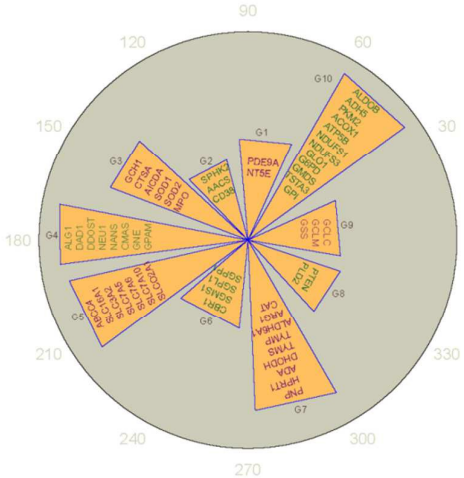

Figure 12 Immunometabolic genes whose depletion could disrupt the balance of $CD4^+$ T cell's metabolism. Those gene were divided into 10

groups depending on their metabolic functions (G1-G10), G1: Fatty acid metabolism; G2: vitamins and signaling molecules; G3: peroxide related reaction; G4: Glycan and aminosugar metabolism; G5: Transporters; G6: Sphingolipid metabolism; G7: Nucleotide metabolism; G8: Phospholipid metabolism; G9: Amino acid metabolism; G10: Glycolysis / Gluconeogenesis, pentose phosphate pathway and other sugars metabolism.

Thus, to have a better understanding of how immunometabolic genes function, we further investigated some of them both metabolically and immunologically. PTEN, the phosphatase and tensin homolog, was showed in details.
PTEN was well known as a tumor suppressor[64-67]. We integrated data from stringDB (http://string-db.org/), KEGG database, and primary literature on PTEN's mechanism and it is shown in Figure 13.

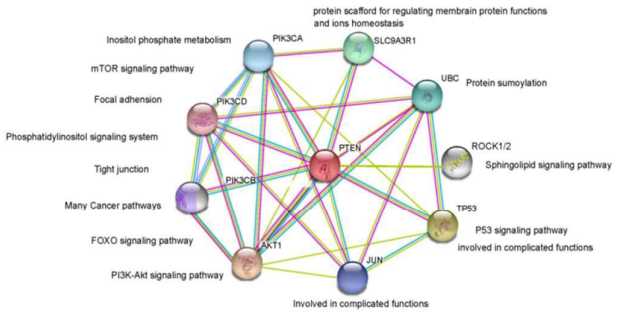

Figure 13 Interaction network of PTEN and its directly interacted proteins expressed in CD4$^+$ T cell. KEGG pathways or related functions were presented to annotate those interactions.

In Figure 13, we saw that most PTEN interaction partners participated in more than one key pathway that was critical in CD4$^+$ T cells. This made PTEN one of the hub proteins in the signaling transduction and transcription regulation system. It also functioned in the activation process of CD4$^+$ T cells to prevent over-stimulation of mTOR signaling pathway and PI3K-Akt signaling pathway to maintain the stability of this cell. At present, metabolic mechanisms of PTEN were mainly presented on liver or adipocyte[68]. And here we would like to penetrate into its metabolic roles in CD4$^+$ T cells by in silico simulation. Firstly, we deleted PTEN in the model, and results showed that, 192 reactions were up-regulated while 280 reactions were down-regulated (supplementary Table 6). And 74 reactions showed changed directions of fluxes compared with control (supplementary Table 6). Those affected reactions cover several metabolic functions. We already know that PTEN is a negative regulator of T cell activation, the same effect of it on tumor progression, since both of them were highly glycolytic. And this was also supported with results of our activation simulation otherwise (data not shown), in which PTEN catalyzed reactions, PI345P3P and PI345P3Pn were both down-regulated. However, inhibiting PTEN also produced features that counter activation. For example, glycolysis was dramatically inhibited with HEX1 was significantly inhibited. But the activity of HEX1 is critical in the activation process[8, 37, 69]. Then, de novo lipogenesis and fatty acid uptake reactions were mostly downregulated, although not dramatic. This was different from the function of PTEN in liver cells[70]. Furthermore, amino acid metabolism and nucleotide metabolism were also disrupted (supplementary Table 6). All those features indicated the disability to activation. Thus, we deduced that, in addition to its signal transduction function, PTEN was indispensible metabolically to maintain systematic balance of T cell and its activation. To test the assumption, we changed the upper bounds of those two reactions (PI345P3P and PI345P3Pn) to 1e-6, to keep them at allowable background level. And we found that the disruption to metabolic system disappeared, which supported our assumption made above.
PTEN has also been proved to be linkage of Treg cell stability and the repression of helper T cell responses[71]. The PTEN-mTORC2 axis was found to be responsible for this function and we proposed that metabolic function of PTEN should also be important in the maintenance of different kinds of T cell subsets' states. With accumulated data on metabolism of those cells, we would disclose detailed mechanisms of PTEN's immunometabolic functions in CD4$^+$ T cell and its subsets in the future.
Based on present understandings of PTEN's functions immunometabolically, inhibiting its activity would disrupt the balance of CD4$^+$ T cells while excessively activating would inhibit the PI3K-Akt-mTOR axis, both of them would disable the activation of naïve CD4$^+$ T cell. So we assumed that PTEN might not be proper to be a drug target for clinical benefits. On one hand, it was widely expressed. And on the other, drugs, either inhibiting or activating of it would cause destructive effects to immune system. Actually, although being a key tumor suppressor, PTEN was not used as a drug target since it was not recorded in the DrugBank database. But its interaction partners showed in Figure 13 were all already taken as drug targets except SLC9A3R1. Worthy of noting was the 3 phosphoinositide 3-kinease isoforms, PIK3CA, PIK3CB and PIK3CD. They were also immunometabolic genes but inhibiting neither of them would disrupt the CD4$^+$ T cell's metabolic network. This not only supported the assumption we made above but also implied that systematic understanding of the functions of a immunometabolic gene would help with the proper selection of drug targets. This logic was applicable to the rest 55 immunometabolic genes identified in this study, and CD4T1670 would be helpful in evaluating the potential of them to be target of certain disease. Also worth mentioning is that we just conducted single gene deletion in this study. Some immunometabolic genes might work with other genes to play critical roles in CD4$^+$ T cells. But this is not the topic of this paper.
In summary, a preliminary trial was conducted to study the immunometabolic mechanisms of CD4$^+$ T cell by computation. PTEN was taken as an example and results showed that it was indispensible in both metabolism and immunity for CD4$^+$ T cells. Worthy of attention is that we didn't integrate CD4T1670 with signaling transduction pathways, but inspected functions of PTEN separately. Thus, it could be only used to simulate the steady state under certain conditions just like other published tissue specific networks[32, 62, 63, 72]. As we know, immunological

signals can regulate the process of metabolism and many metabolites also play critical roles in immunological signaling transduction[6, 7, 34]. So we suggest an integrated method that combines immunity with metabolism to provide more information on specific gene functions and disease progression. For example, this can be reached by constructing an logical model as showed in Oyebode's work[73]. Thus, accumulated knowledge on cross-talk between metabolism and immunity will be sure to help to improve the accuracy of model-based simulation. And the integrated model will contribute to choosing drug targets for certain disease more properly and leading to better clinical output.

Application of CD4T1670 in drug design and drugability evaluation

In DrugBank database, a total of 77 enzyme drug targets (EDTs) (supplementary Table 7) were expressed in $CD4^+$ T cell. We performed single gene deletion for each of the 77 EDTs and found that 34 of them could disrupt the balance of CD4T1670 (supplementary Table 7). Then we extracted drugs that could act on each drug target and this gave us a total of 68 drugs, within which 25 were multi-targets drugs (drug that can act on more than one target). Of the 68 selected drugs, 43 were recorded in SIDER 2, within which 28 were with side effects information. Therefore, we extracted side effects data and the frequency of each immunological associated side effect for each of the 28 drugs (supplementary Table 8). Result showed that 26 kinds of drugs were associated with 493 immunological associated side effect terms. Of those, 18 drugs corresponding to 357 terms were with frequency from 0.30% to 94% or were considered as potential. This indicated that EDTs that could significantly affect the metabolic status of $CD4^+$ T cells might be partly responsible for drugs' induced side effects associated with immune system. Here, we didn't estimate conditions of drugs combination which would result in more entries and more complex results. We neither considered changes from the drugs' target cells that would affect the function of $CD4^+$ T cells. And as the accumulation of drug side effects of uninspected EDTs or by integrating drugs under investigation, we would expect more would be found if off-target occurred to those drugs and $CD4^+$ T cells were affected. Since drug side effects could directly affect the drugability and market of drug target and drugs, we suggest that in future drug design, except for conventional ADMET test, model based evaluation of potential effects of a drug's effects on immune system should be taken into consideration to reduce cost of the whole process.

Conclusions

We reconstructed the metabolic network of human $CD4^+$ T cell, CD4T1670. It is the first metabolic model in the adaptive immune system. We studied in details three critical metabolic subsystems (carbohydrate, glutamine and fatty acid metabolism) in it. Besides features that have been reported by experimental studies, we also gained systematic knowledge of the actions of certain factors and the relationships between different subsystems. Considering that $CD4^+$ T cell is a member in the circulation system, it can sense nutrition status directly. Cellular dependencies on different substrates or genes could be inspected by modulating transport or exchange reactions and performing gene deletions on CD4T1670. With the predicted gene and reaction markers we can guide experimental design and finally more healthy and beneficial dietary plans. As the accumulation of validated tissue-specific metabolic networks, model-based simulations can be used to investigate interactions of multiple tissues or cells. And CD4T1670 is a linkage between those tissues and adaptive immunity. Moreover, it can help with studies on diseases like HIV-1 infection and other immunity-related dysfunctions in human(such as obesity and cancers). To this end, this model can be modified by modulating flux distributions of certain reactions based on available transcriptome or metabonome data of a disease. Lastly, we propose an application of this model in drug or drug target evaluation by inspecting potential side effects of it. And such applications can reduce unnecessary costs in drug design. Importantly, a comprehensive model, integrating metabolic network and immunological signaling pathway, will be more powerful in studies mentioned above. And CD4T1670 has laid the foundation of this target. So we hope that CD4T1670 can spur new knowledge and new assumptions for researchers in the future.

Acknowledgements

This work was supported by the National Basic Research Program of China (Grant No. 2013CB835100), and the National Natural Science Foundation of China (Grant No. 31123005 to J.F.H, No. 31401137 to G.H.L and No. 31401142 to S.X.D.).

references

1. G. Mazzoccoli, S. Carughi, M. Sperandeo, V. Pazienza, F. Giuliani and A. Greco, *Journal of biological regulators and homeostatic agents*, 2011, **25**, 405-416.
2. K. N. Pollizzi and J. D. Powell, *Nature reviews. Immunology*, 2014, **14**, 435-446.
3. T. N. Schumacher, C. Gerlach and J. W. van Heijst, *Nature reviews. Immunology*, 2010, **10**, 621-631.
4. J. J. O'Shea and W. E. Paul, *Science*, 2010, **327**, 1098-1102.
5. D. O'Sullivan and E. L. Pearce, *Trends in immunology*, 2015, **36**, 71-80.
6. R. Wang and D. R. Green, *Nature immunology*, 2012, **13**, 907-915.
7. N. J. MacIver, R. D. Michalek and J. C. Rathmell, *Annual review of immunology*, 2013, **31**, 259-283.
8. E. L. Pearce and E. J. Pearce, *Immunity*, 2013, **38**, 633-643.
9. R. Wang and D. R. Green, *F1000 biology reports*, 2012, **4**, 9.

10. S. J. Bensinger and H. R. Christofk, *Seminars in cell & developmental biology*, 2012, **23**, 352-361.
11. M. G. Vander Heiden, L. C. Cantley and C. B. Thompson, *Science*, 2009, **324**, 1029-1033.
12. I. Samudio, M. Fiegl and M. Andreeff, *Cancer research*, 2009, **69**, 2163-2166.
13. Y. Zheng, G. M. Delgoffe, C. F. Meyer, W. Chan and J. D. Powell, *J Immunol*, 2009, **183**, 6095-6101.
14. I. Chepelev, G. Wei, Q. Tang and K. Zhao, *Nucleic acids research*, 2009, **37**, e106.
15. C. Trapnell, L. Pachter and S. L. Salzberg, *Bioinformatics*, 2009, **25**, 1105-1111.
16. P. De Wit, M. H. Pespeni, J. T. Ladner, D. J. Barshis, F. Seneca, H. Jaris, N. O. Therkildsen, M. Morikawa and S. R. Palumbi, *Molecular ecology resources*, 2012, **12**, 1058-1067.
17. V. Law, C. Knox, Y. Djoumbou, T. Jewison, A. C. Guo, Y. Liu, A. Maciejewski, D. Arndt, M. Wilson, V. Neveu, A. Tang, G. Gabriel, C. Ly, S. Adamjee, Z. T. Dame, B. Han, Y. Zhou and D. S. Wishart, *Nucleic acids research*, 2014, **42**, D1091-1097.
18. M. Kuhn, M. Campillos, I. Letunic, L. J. Jensen and P. Bork, *Molecular systems biology*, 2010, **6**, 343.
19. I. Thiele, N. Swainston, R. M. Fleming, A. Hoppe, S. Sahoo, M. K. Aurich, H. Haraldsdottir, M. L. Mo, O. Rolfsson, M. D. Stobbe, S. G. Thorleifsson, R. Agren, C. Bolling, S. Bordel, A. K. Chavali, P. Dobson, W. B. Dunn, L. Endler, D. Hala, M. Hucka, D. Hull, D. Jameson, N. Jamshidi, J. J. Jonsson, N. Juty, S. Keating, I. Nookaew, N. Le Novere, N. Malys, A. Mazein, J. A. Papin, N. D. Price, E. Selkov, Sr., M. I. Sigurdsson, E. Simeonidis, N. Sonnenschein, K. Smallbone, A. Sorokin, J. H. van Beek, D. Weichart, I. Goryanin, J. Nielsen, H. V. Westerhoff, D. B. Kell, P. Mendes and B. O. Palsson, *Nature biotechnology*, 2013, **31**, 419-425.
20. N. C. Duarte, S. A. Becker, N. Jamshidi, I. Thiele, M. L. Mo, T. D. Vo, R. Srivas and B. O. Palsson, *P Natl Acad Sci USA*, 2007, **104**, 1777-1782.
21. J. Schellenberger, J. O. Park, T. M. Conrad and B. O. Palsson, *BMC bioinformatics*, 2010, **11**, 213.
22. M. Uhlen, L. Fagerberg, B. M. Hallstrom, C. Lindskog, P. Oksvold, A. Mardinoglu, A. Sivertsson, C. Kampf, E. Sjostedt, A. Asplund, I. Olsson, K. Edlund, E. Lundberg, S. Navani, C. A. Szigyarto, J. Odeberg, D. Djureinovic, J. O. Takanen, S. Hober, T. Alm, P. H. Edqvist, H. Berling, H. Tegel, J. Mulder, J. Rockberg, P. Nilsson, J. M. Schwenk, M. Hamsten, K. von Feilitzen, M. Forsberg, L. Persson, F. Johansson, M. Zwahlen, G. von Heijne, J. Nielsen and F. Ponten, *Science*, 2015, **347**, 1260419.
23. M. Uhlen, P. Oksvold, L. Fagerberg, E. Lundberg, K. Jonasson, M. Forsberg, M. Zwahlen, C. Kampf, K. Wester, S. Hober, H. Wernerus, L. Bjorling and F. Ponten, *Nature biotechnology*, 2010, **28**, 1248-1250.
24. A. I. Su, T. Wiltshire, S. Batalov, H. Lapp, K. A. Ching, D. Block, J. Zhang, R. Soden, M. Hayakawa, G. Kreiman, M. P. Cooke, J. R. Walker and J. B. Hogenesch, *P Natl Acad Sci USA*, 2004, **101**, 6062-6067.
25. S. A. Becker and B. O. Palsson, *PLoS computational biology*, 2008, **4**, e1000082.
26. J. Schellenberger, R. Que, R. M. Fleming, I. Thiele, J. D. Orth, A. M. Feist, D. C. Zielinski, A. Bordbar, N. E. Lewis, S. Rahmanian, J. Kang, D. R. Hyduke and B. O. Palsson, *Nature protocols*, 2011, **6**, 1290-1307.
27. A. Bordbar, N. E. Lewis, J. Schellenberger, B. O. Palsson and N. Jamshidi, *Molecular systems biology*, 2010, **6**, 422.
28. K. Breuer, A. K. Foroushani, M. R. Laird, C. Chen, A. Sribnaia, R. Lo, G. L. Winsor, R. E. W. Hancock, F. S. L. Brinkman and D. J. Lynn, *Nucleic acids research*, 2013, **41**, D1228-D1233.
29. S. Bhattacharya, S. Andorf, L. Gomes, P. Dunn, H. Schaefer, J. Pontius, P. Berger, V. Desborough, T. Smith, J. Campbell, E. Thomson, R. Monteiro, P. Guimaraes, B. Walters, J. Wiser and A. J. Butte, *Immunologic research*, 2014, **58**, 234-239.
30. J. D. Orth, I. Thiele and B. O. Palsson, *Nature biotechnology*, 2010, **28**, 245-248.
31. J. M. Toung, M. Morley, M. Li and V. G. Cheung, *Genome research*, 2011, **21**, 991-998.
32. A. Bordbar, N. E. Lewis, J. Schellenberger, B. O. Palsson and N. Jamshidi, *Molecular systems biology*, 2010, **6**.
33. A. Mardinoglu, R. Agren, C. Kampf, A. Asplund, I. Nookaew, P. Jacobson, A. J. Walley, P. Froguel, L. M. Carlsson, M. Uhlen and J. Nielsen, *Molecular systems biology*, 2013, **9**, 649.
34. V. A. Gerriets and J. C. Rathmell, *Trends in immunology*, 2012, **33**, 168-173.
35. W. H. Koppenol, P. L. Bounds and C. V. Dang, *Nature reviews. Cancer*, 2011, **11**, 325-337.
36. K. A. Frauwirth, J. L. Riley, M. H. Harris, R. V. Parry, J. C. Rathmell, D. R. Plas, R. L. Elstrom, C. H. June and C. B. Thompson, *Immunity*, 2002, **16**, 769-777.
37. A. N. Macintyre, V. A. Gerriets, A. G. Nichols, R. D. Michalek, M. C. Rudolph, D. Deoliveira, S. M. Anderson, E. D. Abel, B. J. Chen, L. P. Hale and J. C. Rathmell, *Cell Metab*, 2014, **20**, 61-72.
38. T. Eleftheriadis, G. Pissas, A. Karioti, G. Antoniadi, N. Antoniadis, V. Liakopoulos and I. Stefanidis, *Journal of basic and clinical physiology and pharmacology*, 2013, **24**, 271-276.
39. L. Berod, C. Friedrich, A. Nandan, J. Freitag, S. Hagemann, K. Harmrolfs, A. Sandouk, C. Hesse, C. N. Castro, H. Bahres, S. K. Tschirner, N. Gorinski, M. Gohmert, C. T. Mayer, J. Huehn, E. Ponimaskin, W. R. Abraham, R. Muller, M. Lochner and T. Sparwasser, *Nat Med*, 2014, **20**, 1327-1333.
40. M. S. Ardawi, *Metabolism: clinical and experimental*, 1988, **37**, 99-103.
41. E. L. Carr, A. Kelman, G. S. Wu, R. Gopaul, E. Senkevitch, A. Aghvanyan, A. M. Turay and K. A. Frauwirth, *J Immunol*, 2010, **185**, 1037-1044.

42. L. V. Sinclair, J. Rolf, E. Emslie, Y. B. Shi, P. M. Taylor and D. A. Cantrell, *Nature immunology*, 2013, **14**, 500-508.
43. R. Stern, A. A. Asari and K. N. Sugahara, *European journal of cell biology*, 2006, **85**, 699-715.
44. P. L. Bollyky, J. D. Lord, S. A. Masewicz, S. P. Evanko, J. H. Buckner, T. N. Wight and G. T. Nepom, *J Immunol*, 2007, **179**, 744-747.
45. A. J. Day and C. A. de la Motte, *Trends in immunology*, 2005, **26**, 637-643.
46. M. Schlemmer, U. Suchner, B. Schapers, E. M. Duerr, B. Alteheld, T. Zwingers, P. Stehle and H. G. Zimmer, *Clin Nutr*, 2015, DOI: 10.1016/j.clnu.2014.12.021.
47. V. F. Cruzat, M. M. Rogero and J. Tirapegui, *Cell biochemistry and function*, 2010, **28**, 24-30.
48. K. D. Singleton and P. E. Wischmeyer, *Biochemical and biophysical research communications*, 2008, **373**, 445-449.
49. H. M. Ko, N. I. Kang, Y. S. Kim, Y. M. Lee, Z. W. Jin, Y. J. Jung, S. Y. Im, J. H. Kim, Y. H. Shin, B. H. Cho and H. K. Lee, *Clinical and experimental allergy : journal of the British Society for Allergy and Clinical Immunology*, 2008, **38**, 357-364.
50. C. Varol, I. Zvibel, L. Spektor, F. D. Mantelmacher, M. Vugman, T. Thurm, M. Khatib, E. Elmaliah, Z. Halpern and S. Fishman, *J Immunol*, 2014, **193**, 4002-4009.
51. D. B. Ballak, R. Stienstra, A. Hijmans, L. A. Joosten, M. G. Netea and C. J. Tack, *Cytokine*, 2013, **62**, 96-103.
52. S. E. Shoelson and A. B. Goldfine, *Nat Med*, 2009, **15**, 373-374.
53. J. Lee, M. C. Walsh, K. L. Hoehn, D. E. James, E. J. Wherry and Y. Choi, *J Immunol*, 2014, **192**, 3190-3199.
54. M. Lochner, L. Berod and T. Sparwasser, *Trends in immunology*, 2015, **36**, 81-91.
55. M. I. Malandrino, R. Fucho, M. Weber, M. Calderon-Dominguez, J. F. Mir, L. Valcarcel, X. Escote, M. Gomez-Serrano, B. Peral, L. Salvado, S. Fernandez-Veledo, N. Casals, M. Vazquez-Carrera, F. Villarroya, J. J. Vendrell, D. Serra and L. Herrero, *American journal of physiology. Endocrinology and metabolism*, 2015, **308**, E756-769.
56. M. Schrader and H. D. Fahimi, *Biochimica et biophysica acta*, 2006, **1763**, 1755-1766.
57. J. A. Hollenbaugh, J. Munger and B. Kim, *Virology*, 2011, **415**, 153-159.
58. L. J. Sitole, A. A. Williams and D. Meyer, *Molecular bioSystems*, 2013, **9**, 18-28.
59. E. W. Taylor, *Toxicology*, 2010, **278**, 124-130.
60. S. T. Chang, P. Sova, X. Peng, J. Weiss, G. L. Law, R. E. Palermo and M. G. Katze, *mBio*, 2011, **2**.
61. L. Jerby, T. Shlomi and E. Ruppin, *Molecular systems biology*, 2010, **6**, 401.
62. Y. Zhao and J. Huang, *Biochemical and biophysical research communications*, 2011, **415**, 450-454.
63. A.-D. Zhang, S.-X. Dai and J.-F. Huang, *BioMed research international*, 2013, **2013**.
64. F. Molinari and M. Frattini, *Frontiers in oncology*, 2013, **3**, 326.
65. S. Phin, M. W. Moore and P. D. Cotter, *Frontiers in oncology*, 2013, **3**, 240.
66. T. D. Bunney and M. Katan, *Nature reviews. Cancer*, 2010, **10**, 342-352.
67. N. Chalhoub and S. J. Baker, *Annual review of pathology*, 2009, **4**, 127-150.
68. G. P. Lobo, K. A. Waite, S. M. Planchon, T. Romigh, J. A. Houghton and C. Eng, *Human molecular genetics*, 2008, **17**, 2877-2885.
69. R. D. Michalek, V. A. Gerriets, S. R. Jacobs, A. N. Macintyre, N. J. MacIver, E. F. Mason, S. A. Sullivan, A. G. Nichols and J. C. Rathmell, *J Immunol*, 2011, **186**, 3299-3303.
70. M. Peyrou, L. Bourgoin, A. L. Poher, J. Altirriba, C. Maeder, A. Caillon, M. Fournier, X. Montet, F. Rohner-Jeanrenaud and M. Foti, *Journal of hepatology*, 2015, **62**, 421-429.
71. S. Shrestha, K. Yang, C. Guy, P. Vogel, G. Neale and H. Chi, *Nature immunology*, 2015, **16**, 178-187.
72. C. Gille, C. Bolling, A. Hoppe, S. Bulik, S. Hoffmann, K. Hubner, A. Karlstadt, R. Ganeshan, M. Konig, K. Rother, M. Weidlich, J. Behre and H. G. Holzhutter, *Molecular systems biology*, 2010, **6**, 411.
73. O. J. Oyeyemi, O. Davies, D. L. Robertson and J. M. Schwartz, *Bioinformatics*, 2015, **31**, 1075-1083.